ChemComm

ROYAL SOCIETY OF CHEMISTRY

COMMUNICATION

View Article Online
View Journal | View Issue

Check for updates

Cite this: *Chem. Commun.*, 2018, 54, 12186

Received 5th September 2018,
Accepted 4th October 2018

DOI: 10.1039/c8cc07207h

rsc.li/chemcomm

Assisted π-stacking: a strong synergy between weak interactions†

Soumik Sao,[a] Sumit Naskar,[a] Narottam Mukhopadhyay,[a] Mousumi Das*[ab] and Debangshu Chaudhuri*[ab]

Synergy between a pair of weak non-covalent interactions can predispose a molecular self-assembly towards a specific pathway. We report assisted π-stacking, a synergy between aromatic π-stacking and n → π* interactions that exhibits an unprecedented strength and thermal stability. Natural bond orbital analysis reveals the non-additive nature of the interaction.

The properties of a molecular self-assembly are governed by how its constituent molecules are organized. Unlike covalent bonding that involves orbital overlap and is therefore strongly directional in nature, non-covalent interactions impose much relaxed orientational restrictions.[1] While such freedom allows one to create a variety of assembled structures from the same building blocks, it also presents an inherent challenge in terms of guiding a self-assembly through a specific pathway, to a desired structure.[2,3]

Control over the self-assembly pathway is achieved by exploiting a very unique feature of non-covalent interactions, namely the non-additivity.[4] Non-additivity governs the way in which non-covalent interactions mutually strengthen (or weaken) each other, and can in turn bias the course of a self-assembly.[3,5] Such mutual strengthening is manifested in two related, but somewhat distinct ways: cooperativity and synergy. The former is usually a many-body effect, operating through multiple short- and long-range interactions,[6,7] and is commonly encountered in large hydrogen-bonded systems.[8] Synergy on the other hand, is a pair or reciprocal effect, where two non-covalent interactions complement each other such that the resultant association is stronger than the sum of individual interactions.[9] A strong synergistic interaction can locally influence the self-assembled structure by favouring certain arrangements over the others,[10] and can even be a precursor to cooperativity. From the point of view of molecular design, it is easier to incorporate a synergistic pair of interactions, as opposed to aiming for cooperativity through a fortuitous interplay of multiple interactions.

We report an unusually strong synergistic interaction between regular aromatic π-stacking and a much weaker n → π* interaction. The participation of the secondary n → π* interaction is so critical that switching it off has the dramatic effect of disrupting the otherwise stable pi-stacked state. This synergistic interaction, which we refer to as assisted π-stacking, exhibits an extraordinary strength and thermal stability hitherto unprecedented among the strongest pi-stacked systems.

Fig. 1a presents the molecules under investigation. **Py-2NDI** and **Py-2PBI** are covalently bridged dimers of naphthalene diimide (NDI) and perylene bisimide (PBI), respectively. Free rotations around the methylene carbons of the bridging 2,6-lutidinyl group allow **Py-2NDI** (and **Py-2PBI**) to switch between open and folded conformations. Unlike the open conformer, where the two NDI (PBI) chromophores are far removed and therefore non-interacting, the folded conformer can support two distinct non-covalent interactions: π-stacking between the NDI (PBI) units, and a donor–acceptor type interaction between the pyridyl N lone pair and the two electron-deficient NDI (PBI) moieties. The **mX-2NDI** and **mX-2PBI** dimers on the other hand, can only support π-stacking,[11,12] and therefore serve as negative controls.

We carried out an in-depth investigation of the electronic and structural aspects of dimer folding, in order to understand the nature of the interaction that drives it. Fig. 1b presents the optical absorption spectrum of **Py-2NDI** vis-à-vis that of **mX-2NDI**, in $CHCl_3$. The spectrum of **mX-2NDI** exhibits typical characteristics of an isolated NDI chromophore: 0–0, 0–1 and 0–2 vibronic bands appearing at 380, 360 and 340 nm, respectively.[21] Evidently, in a "good" solvent such as $CHCl_3$, the control dimer assumes a non-interacting, open conformation. In contrast, the spectrum of **Py-2NDI** is marked by a distinctly diminished absorbance at the 0–0 band (A_{0-0}). The corresponding decrease in the 0–0 to 0–1 absorbance ratio, A_{0-0}/A_{0-1} from 1.13 to 0.96 is a tell-tale sign of an H-type excitonic coupling.[13]

---

[a] *Department of Chemical Sciences, Indian Institute of Science Education and Research (IISER) Kolkata, Mohanpur 741246, India. E-mail: dchaudhuri@iiserkol.ac.in*

[b] *Centre for Advanced Functional Materials (CAFM), Indian Institute of Science Education and Research (IISER) Kolkata, Mohanpur 741246, India*

† Electronic supplementary information (ESI) available: Experimental methods, synthesis and characterization, and additional figures. See DOI: 10.1039/c8cc07207h

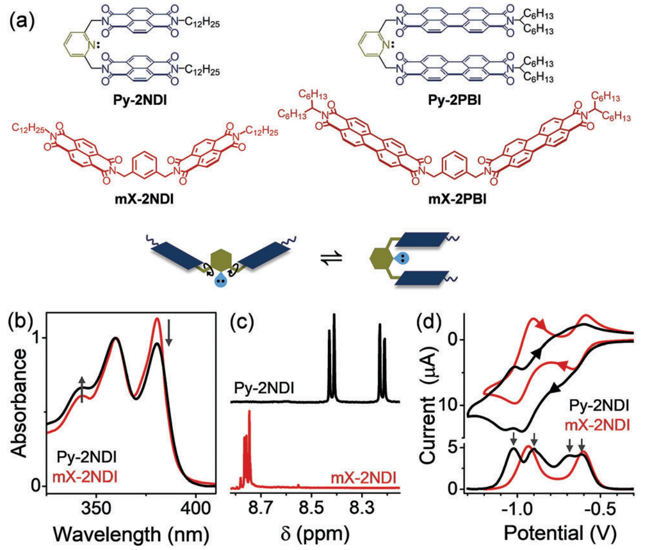

Fig. 1 (a) Molecular structures of **Py-2NDI** and **Py-2PBI**, and the respective control dimers **mX-2NDI** and **mX-2PBI**. The schematic represents the dynamic folding equilibrium of the dimers. A comparison based on (b) normalized optical absorption spectra (~50 μM, normalized at A_{0-1}), (c) the aromatic region of the ^{1}H-NMR spectra, and (d) CV (~10 μM) at 0.1 V s^{-1} scan rate *vs.* saturated calomel electrode in $CHCl_3$ confirms the presence of excitonic, structural and electronic interactions between the two NDI units in folded **Py-2NDI**, as opposed to **mX-2NDI** that exists as the open conformer. DPV of the two NDI dimers is shown at the bottom of panel (d).

Identical spectra at high levels of dilution implies that the observed phenomenon is purely intramolecular (Fig. S4, ESI†), resulting from a folded conformation in which two NDI units are cofacially stacked. This observation is particularly surprising since NDI π-stacking is strongly disfavored in $CHCl_3$ (association constant <1 M^{-1}).[14] While optical absorption spectroscopy provides a reliable way to monitor the nature and strength of exciton coupling between NDI chromophores in the folded state, ^{1}H-NMR spectroscopy provides an independent investigation of the structural interactions in different dimer conformations. Fig. 1c presents the aromatic region of ^{1}H-NMR spectra of the two dimers in $CDCl_3$. The eight NDI protons of **mX-2NDI** give rise to a multiplet signal at 8.75 ppm, their chemical shift consistent with that of an unstacked, isolated NDI.[15,16] The NDI protons of **Py-2NDI**, on the other hand, are strongly upfield shifted, appearing as two sets of doublets at 8.21 and 8.41 ppm. Such a strong shielding of NDI protons in **Py-2NDI** is a clear evidence of π-stacking in the folded state.[15,16] Furthermore, two sets of doublets indicate a rotational displacement of one NDI with respect to the other in the folded geometry, such that one half of the NDI protons are shielded better than the other half. This is in perfect agreement with the geometry-optimized structure of the **Py-2NDI** dimer, discussed subsequently. A similar comparison of **Py-2PBI** vis-à-vis its negative control **mX-2PBI** confirms the generality of the observed phenomenon (Fig. S6, ESI†).

Cyclic voltammetry in $CHCl_3$ (Fig. 1d) elegantly captures the difference between **Py-2NDI** and **mX-2NDI** dimer conformations, in terms of the extent of electronic interactions between the two NDI units, and how the folded dimer responds to a stepwise electrochemical reduction. The cyclic voltammogram (CV) of **mX-2NDI** is characterized by two reversible, one-electron reduction waves, appearing at $E_{1/2}(1) = -626$ and $E_{1/2}(2) = -959$ mV. This redox behavior is consistent with the open conformation of the **mX-2NDI** dimer, where each NDI unit is independently and identically reduced in two distinct steps, to a $[\text{NDI}]^{\bullet-}$ radical anion and eventually to a $[\text{NDI}]^{2-}$ dianion.[16] Identical values of the faradaic current peaks in the differential pulse voltammogram (DPV) confirm the sequence of these single-electron reduction events. In contrast, **Py-2NDI** exhibits a distinctly irreversible CV. A pair of strongly interacting NDIs is expected to undergo four discrete one-electron reduction steps.[16] These individual reduction events are better resolved in the DPV of **Py-2NDI**, appearing at −612, −684, −900 and −1024 mV *vs.* SCE. The potential difference between the first two cathodic peaks that gives a measure of e–e repulsion within the dianion, is drastically reduced from 333 mV in open **mX-2NDI** to 72 mV in folded **Py-2NDI**. A strong electronic coupling between the two NDI units of the folded **Py-2NDI** helps to delocalize the dianion state over the dimer, resulting in a reduced coulombic repulsion. Upon further reduction, the repulsion becomes strong enough to destabilize the folded state, causing a conformational change, and resulting in an irreversible CV.[17]

The results presented so far clearly establish that the **Py-2NDI** (and **Py-2PBI**) exists in the intramolecularly pi-stacked folded form in $CHCl_3$, while the structurally similar **mX-2NDI** (and **mX-2PBI**) dimer assumes the open conformation. In order to elucidate the nature of this unusual π-stacking interaction in 2,6-lutidinyl bridged dimers and the role of the pyridyl N lone pair, we carried out a protonation based experiment. The aim was to turn-off any lone pair mediated interaction,‡ and monitor its influence on the dimer conformation, using the same set of experiments as before. Fig. 2a (and Fig. S6a, ESI†) presents the effect on the optical absorption spectra, in $CHCl_3$. Upon protonation, the A_{0-0}/A_{0-1} ratio increases from 0.96 to 1.22, signifying a change from the intramolecularly folded H-aggregate to the non-interacting open form. Interestingly, the effect of protonation is fully reversible, as adding a base (triethylamine, Et_3N) frees up the pyridyl N lone pair and restores the H-aggregated dimer spectrum. Clearly the availability of the pyridyl N lone pair is critical to the stability of the pi-stacked folded dimer in $CHCl_3$, which cannot be achieved otherwise through π-stacking alone. In the ^{1}H-NMR spectrum, two sets of NDI aromatic protons of folded **Py-2NDI** experience a pronounced downfield shift upon protonation (Fig. 2b and Fig. S5, S6b, ESI† for **Py-2PBI**), giving rise to a complex multiplet signal at 8.76 ppm, similar to that of NDI protons of the open **mX-2NDI** dimer. Once again, deprotonation using Et_3N restores the original ^{1}H-NMR spectrum. Even cyclic voltammetry of the protonated **Py-2NDI** (Fig. 2c) reproduces to a great extent, the characteristic features of the non-interacting, open dimer: a reversible CV with a pair of one-electron reduction peaks, separated by 365 mV.

In order to unravel the exact nature of the lone-pair assisted π-stacking interaction, natural bond orbital (NBO) analysis was performed on the optimized dimer structure. Quite consistent

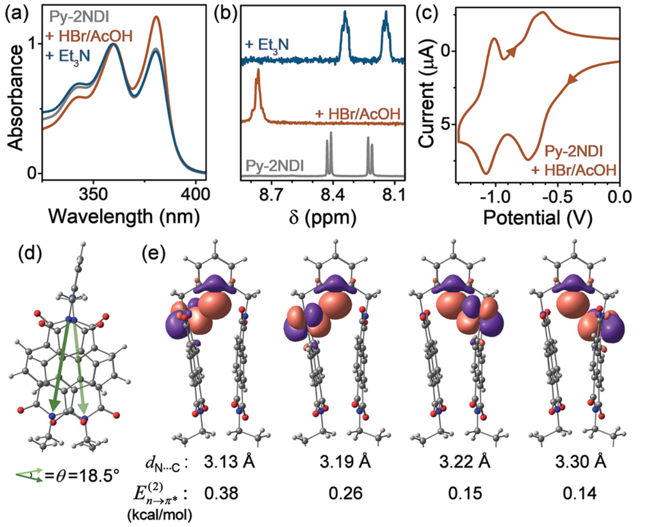

Fig. 2 Lone pair assisted π-stacking. Protonation at the pyridyl N (using HBr/acetic acid) causes changes in the (a) A_{0-0}/A_{0-1} ratio, and (b) deshielding of NDI aromatic protons, consistent with dimer unfolding. In both experiments, a subsequent deprotonation (using Et_3N, blue curves) restores the original spectrum. (c) CV of protonated **Py-2NDI** closely resembles that of the open **mX-2NDI**. (d) Geometry optimized structure of folded **Py-2NDI** confirms a ∼19° rotational displacement between the two NDI units. Green arrows represent the NDI transition dipole moments; n-$C_{12}H_{25}$ groups are truncated for clarity. (e) NBO analysis confirms $n_N \rightarrow \pi_{C=O}^*$ interactions between the pyridyl N and NDI carbonyl groups. N⋯C interaction distances ($d_{N\cdots C}$) and the calculated interaction energies ($E^{(2)}_{n\rightarrow\pi^*}$) are noted.

with the results so far, folded conformers of **Py-2NDI** (and **Py-2PBI**) represent the lowest-energy conformations (Fig. 2d and Fig. S7, ESI†), with the shortest separation between the NDI chromophores being under 3.3 Å (Fig. S8, ESI†). In the folded state, one NDI unit is rotationally displaced (θ ∼ 19°) with respect to the other, making one half of the NDI protons chemically distinct from the other half. This accounts for the observed split doublet feature (at 8.21 and 8.41 ppm) in the ^{1}H-NMR spectrum, described earlier. Interestingly, in the folded conformation, the pyridyl N is in close proximity to the four carbonyl carbons, such that the corresponding N⋯C distances ($d_{N\text{–}C}$ ∼ 3.13–3.3 Å) are either smaller than or comparable to the sum of van der Waals radii (3.25 Å). NBO overlaps between the pyridyl N lone pair (n_N) and each of the four $\pi_{C=O}^*$, shown in Fig. 2e, confirm the presence of significant n → π* interactions in the folded conformation.[10,18,19] Further evidence in favour of n → π* interaction comes from NBO deletion analysis (Table S1, ESI†), wherein deletion of the said interaction increases electron occupancy at the donor N atom. Individual strength of these n → π* interactions, estimated from the second order perturbation energies ($E^{(2)}_{n\rightarrow\pi^*}$), are in the order of 0.14–0.38 kcal mol^{-1} (0.1–0.45 kcal mol^{-1} for **Py-2PBI**), and are comparable with the reported values.[10,19] It is surprising that a single lone pair donor (n_N) engaging simultaneously with 4 different carbonyl acceptors ($\pi_{C=O}^*$) can result in reasonably strong n → π* interactions. The confidence in our findings is further bolstered by the fact that the two control dimers (**mX-2NDI** and **mX-2PBI**) do not support any secondary non-covalent interaction§ other than regular π-stacking (Fig. S8, ESI†), thus highlighting the critical role of the pyridyl N lone pair in assisted π-stacking.

A comparison of the energy difference between folded and open conformers of **Py-2NDI** and **mX-2NDI** dimers reveals the non-additive nature of assisted π-stacking interactions (Fig. S7, ESI†). While the folded conformer is more stable in both cases, the extent of stabilization is greater in the case of assisted pi-stacked **Py-2NDI** by 3.86 kcal mol^{-1}. Interestingly, this difference is much higher than what can be accounted for by the four $n_N \rightarrow \pi_{C=O}^*$ interactions (cumulative $E^{(2)}_{n\rightarrow\pi^*} = 0.93$ kcal mol^{-1}). Thus $n_N \rightarrow \pi_{C=O}^*$ assisted π-stacking interaction is much stronger than what is expected from a simple algebraic sum of $n_N \rightarrow \pi_{C=O}^*$ and π-stacking interactions. Though PBI is known to exhibit a stronger π-stacking than NDI, the assisted π-stacking interaction in **Py-2NDI** is comparatively stronger ($\Delta\Delta E_{A\pi S} = -3.86$ kcal mol^{-1}) than that in **Py-2PBI** ($\Delta\Delta E_{A\pi S} = -3.24$ kcal mol^{-1}, Fig. S7, ESI†). This too is consistent with the idea of non-additivity: strong individual interactions do not necessarily give rise to a stronger synergy.

That the strength of n → π* assisted π-stacking in **Py-2NDI** and **Py-2PBI** far exceeds that of a regular π-stacking is also realized experimentally, from its extraordinary thermal stability in solution. The optical absorption spectra of **Py-2NDI** (and **Py-2PBI**) in non-aggregating solvents, such as chlorobenzene at 125 °C (Fig. S9, ESI†) and DMSO at 180 °C (Fig. 3), are virtually indistinguishable from the corresponding spectra at room temperature. This is in sharp contrast to a vast majority of pi-stacked aggregates of NDI[20] and PBI,[7,12,21] which experience a pronounced disassembly between 50 and 100 °C, even those which are cooperatively bound and/or are supplemented by stronger side-group interactions, such as H-bonding. It is remarkable that $n_N \rightarrow \pi_{C=O}^*$ interaction, despite being more than an order of magnitude weaker than π-stacking, can strengthen the latter to such unprecedented levels. This, once again, highlights the non-additive nature of assisted π-stacking.

In conclusion, we have identified a unique class of assisted π-stacking interaction that is born out of a strong synergy between two weak interactions: π-stacking and n → π* interactions. The resultant association is so strong that it not only forms readily in a non-aggregating medium such as $CHCl_3$, but also remains exceptionally stable at elevated temperatures. The significance of

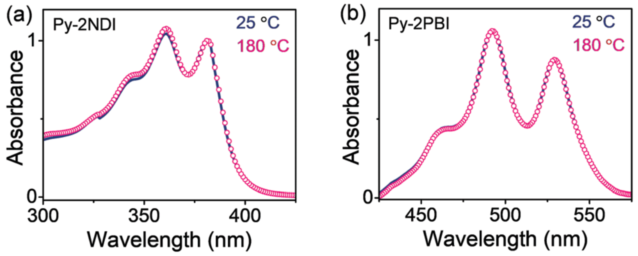

Fig. 3 n → π* assisted π-stacking in folded (a) **Py-2NDI** and (b) **Py-2PBI** exhibit extraordinary thermal stability, up to 180 °C in non-aggregating DMSO. Normalized optical absorption spectra remain unchanged at higher temperatures.

this finding should be seen in the light of the fact that the strength of such assisted π-stacking interaction surpasses all known pi-stacked aggregates of NDI and PBI. We believe the key to a strong synergy lies in a judicious organization of the two non-covalent interaction motifs, the π-stacking NDI/PBI unit and the position of the lone-pair bearing N atom. In **Py-2NDI** and **Py-2PBI** folda-dimers, this is achieved by having the pyridyl N atom flanked between two arylene diimide units, such that the π-stacking and $n_N \rightarrow \pi_{C=O}^*$ interactions could mutually consolidate each other in the folded conformer. Such strong synergistic interactions are great tools to exercise pathway control in molecular self-assembly, and can also find potential use in supramolecular catalysis by stabilizing the transition state.[22]

The authors gratefully acknowledge Department of Science and Technology (DST), India (Project: EMR/2014/000223 and SB/FT/CS-164/2013) for financial support. S. S. and N. M. acknowledge UGC, and S. N. thanks IISER-K for a scholarship.

Conflicts of interest

There are no conflicts to declare.

Notes and references

‡ While pyridyl N protonation primarily causes the termination of the $n_N \rightarrow \pi_{C=O}^*$ interaction, it also changes the chemical environment of the molecule, changing it from a neutral to a charged species.

§ In the folded conformer of **mX-dimers**, the shortest distance between the proton at the C2 position of the bridging m-xylylene ring and the closest carbonyl O or C atoms is larger than the sum of van der Waals radii. This rules out any stabilising C–H···O or destabilizing steric interaction.

1 P. Kollman, *Acc. Chem. Res.*, 1977, **10**, 365; L. Brunsveld, B. J. B. Folmer, E. W. Meijer and R. P. Sijbesma, *Chem. Rev.*, 2001, **101**, 4071.
2 A. Lohr, M. Lysetska and F. Würthner, *Angew. Chem., Int. Ed.*, 2005, **44**, 5071; P. Jonkheijm, P. van der Schoot, A. P. H. J. Schenning and E. W. Meijer, *Science*, 2006, **313**, 80.
3 P. A. Korevaar, S. J. George, A. J. Markvoort, M. M. J. Smulders, P. A. J. Hilbers, A. P. H. J. Schenning, T. F. A. De Greef and E. W. Meijer, *Nature*, 2012, **481**, 492.
4 P. L. Huyskens, *J. Am. Chem. Soc.*, 1977, **99**, 2578; C. Farina, F. C. Santos and A. C. Tort, *Am. J. Phys.*, 1999, **67**, 344; C. Biot, R. Wintjens and M. Rooman, *J. Am. Chem. Soc.*, 2004, **126**, 6220.
5 T. E. Kaiser, V. Stepanenko and F. Würthner, *J. Am. Chem. Soc.*, 2009, **131**, 6719; J. Kang, D. Miyajima, T. Mori, Y. Inoue, Y. Itoh and T. A. Aida, *Science*, 2015, **347**, 646; M. Endo, T. Fukui, S. H. Jung, S. Yagai, M. Takeuchi and K. Sugiyasu, *J. Am. Chem. Soc.*, 2016, **138**, 14347; S. Ogi, K. Matsumoto and S. Yamaguchi, *Angew. Chem., Int. Ed.*, 2018, **57**, 2339.
6 M. J. Elrod and R. J. Saykally, *Chem. Rev.*, 1994, **94**, 1975; B. Rybtchinski, *ACS Nano*, 2011, **5**, 6791; A. S. Mahadevi and G. N. Sastry, *Chem. Rev.*, 2016, **116**, 2775.
7 C. Kulkarni, K. K. Bejagam, S. P. Senanayak, K. S. Narayan, S. Balasubramanian and S. J. George, *J. Am. Chem. Soc.*, 2015, **137**, 3924.
8 R. P. Sijbesma, F. H. Beijer, L. Brunsveld, B. J. B. Folmer, J. H. K. K. Hirschberg, R. F. M. Lange, J. K. L. Lowe and E. W. Meijer, *Science*, 1997, **278**, 1601.
9 D. Vijay and G. N. Sastry, *Chem. Phys. Lett.*, 2010, **485**, 235; O. Perraud, V. Robert, H. Gornitzka, A. Martinez and J. Dutasta, *Angew. Chem., Int. Ed.*, 2012, **51**, 504.
10 A. Rahim, P. Saha, K. K. Jha, N. Sukumar and B. K. Sarma, *Nat. Commun.*, 2017, **8**, 78.
11 S. Sao, B. R. Samanta and D. Chaudhuri, *RSC Adv.*, 2016, **6**, 34350.
12 S. Samanta and D. Chaudhuri, *J. Phys. Chem. Lett.*, 2017, **8**, 3427.
13 F. C. Spano, *Acc. Chem. Res.*, 2010, **43**, 429.
14 M. S. Cubberley and B. L. Iverson, *J. Am. Chem. Soc.*, 2001, **123**, 7560.
15 C. Shao, M. Grüne, M. Stolte and F. Würthner, *Chem. – Eur. J.*, 2012, **18**, 13665.
16 Y. Wu, M. Frasconi, D. M. Gardner, P. R. McGonigal, S. T. Schneebeli, M. R. Wasielewski and J. F. Stoddart, *Angew. Chem., Int. Ed.*, 2014, **53**, 9476.
17 F. Schlosser, M. Moos, C. Lambert and F. Würthner, *Adv. Mater.*, 2013, **25**, 410; A. Takai, T. Yasuda, T. Ishizuka, T. Kojima and M. Takeuchi, *Angew. Chem., Int. Ed.*, 2013, **52**, 9167.
18 M. Egli and S. Sarkhel, *Acc. Chem. Res.*, 2007, **40**, 197; B. C. Gorske, B. L. Bastian, G. D. Geske and H. E. Blackwell, *J. Am. Chem. Soc.*, 2007, **129**, 8928; A. Choudhary, D. Gandla, G. R. Krow and R. T. Raines, *J. Am. Chem. Soc.*, 2009, **131**, 7244.
19 S. K. Singh, K. K. Mishra, N. Sharma and A. Das, *Angew. Chem., Int. Ed.*, 2016, **55**, 7801.
20 M. R. Molla and S. Ghosh, *Chem. Mater.*, 2011, **23**, 95; A. Sikder, A. Das and S. Ghosh, *Angew. Chem., Int. Ed.*, 2015, **54**, 6755.
21 S. Ogi, V. Stepanenko, K. Sugiyasu, M. Takeuchi and F. Würthner, *J. Am. Chem. Soc.*, 2015, **137**, 3300.
22 Y. Zhao, Y. Domoto, E. Orentas, C. Beuchat, D. Emery, J. Mareda, N. Sakai and S. Matile, *Angew. Chem., Int. Ed.*, 2013, **52**, 9940.